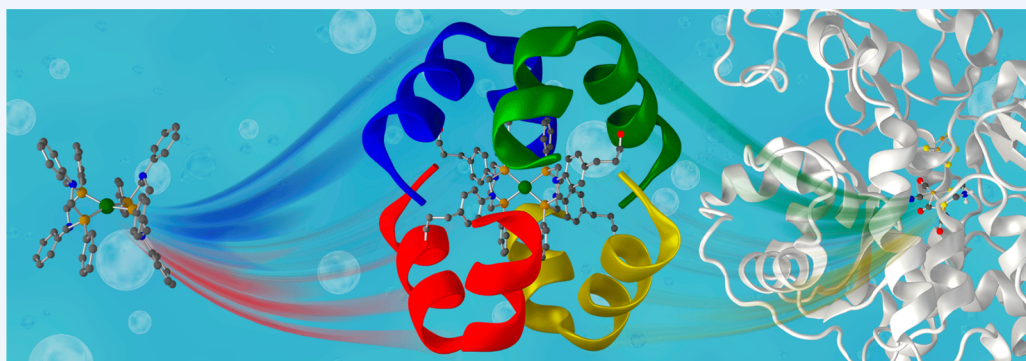


Beyond the Active Site: The Impact of the Outer Coordination Sphere on Electrocatalysts for Hydrogen Production and Oxidation

Bojana Ginovska-Pangovska, Arnab Dutta, Matthew L. Reback, John C. Linehan, and Wendy J. Shaw*

Pacific Northwest National Laboratory, Richland, Washington 99354, United States



CONSPECTUS: Redox active metalloenzymes play a major role in energy transformation reactions in biological systems. Examples include formate dehydrogenases, nitrogenases, CO dehydrogenase, and hydrogenases. Many of these reactions are also of interest to humans as potential energy storage or utilization reactions for photoelectrochemical, electrolytic, and fuel cell applications. These metalloenzymes consist of redox active metal centers where substrates are activated and undergo transformation to products accompanied by electron and proton transfer to or from the substrate. These active sites are typically buried deep within a protein matrix of the enzyme with channels for proton transport, electron transport, and substrate/product transport between the active site and the surface of the protein. In addition, there are amino acid residues that lie in close proximity to the active site that are thought to play important roles in regulating and enhancing enzyme activity. Directly studying the outer coordination sphere of enzymes can be challenging due to their complexity, and the use of modified molecular catalysts may allow us to provide some insight. There are two fundamentally different approaches to understand these important interactions. The “bottom-up” approach involves building an amino acid or peptide containing outer coordination sphere around a functional molecular catalyst, and the “top-down” approach involves attaching molecular catalyst to a structured protein. Both of these approaches have been undertaken for hydrogenase mimics and are the emphasis of this Account.

Our focus has been to utilize amino acid or peptide based scaffolds on an active functional enzyme mimic for H₂ oxidation and production, [Ni(P^R₂N^{R'}₂)₂]²⁺. This “bottom-up” approach has allowed us to evaluate individual functional group and structural contributions to electrocatalysts for H₂ oxidation and production. For instance, using amine, ether, and carboxylic acid functionalities in the outer coordination sphere enhances proton movement and results in lower catalytic overpotentials for H₂ oxidation, while achieving water solubility in some cases. Amino acids with acidic and basic side chains concentrate substrate around catalysts for H₂ production, resulting in up to 5-fold enhancements in rate. The addition of a structured peptide in an H₂ production catalyst limited the structural freedom of the amino acids nearest the active site, while enhancing the overall rate. Enhanced stability to oxygen or extreme conditions such as strongly acidic or basic conditions has also resulted from an amino acid based outer coordination sphere.

From the “top-down” approach, others have achieved water solubility and photocatalytic activity by associating this core complex with photosystem-I. Collectively, by use of this well understood core, the role of individual and combined features of the outer coordination sphere are starting to be understood at a mechanistic level. Common mechanisms have yet to be defined to predictably control these processes, but our growing knowledge in this area is essential for the eventual mimicry of enzymes by efficient molecular catalysts for practical use.

■ INTRODUCTION

Enzymes play critical roles in executing chemical transformations in nature through subtle, synchronized interactions between the protein and the substrate. Metalloenzymes typically consist of a relatively small metal-containing active site where the chemical transformations occur, surrounded by

an outer coordination sphere consisting of the amino acids in the protein scaffold. Chemical transformations by enzymes are typically much more efficient than molecular catalyst models

Received: April 29, 2014

Published: June 19, 2014

which focus solely upon the active site. This nearly universal observation suggests that including features from the protein scaffold may be necessary to produce a catalyst with comparable activity.

The protein scaffold of enzymes has been demonstrated to contribute significantly to catalyst specificity, selectivity, and efficiency.^{1–4} One of the most essential functions of the scaffold is to deliver substrates and products to and from the buried active site. This is accomplished through channels, which provide spatial and temporal control of the delivery.^{2,4} In addition to shuttling reactants and products, the environment created around the active site serves to finely tune the reactivity. This is achieved by positioning the diverse backbone and functional groups in the surrounding protein scaffold to precisely define the chirality, dielectric, polarity, charge, and hydrogen bonding around the active site at the molecular level.³ Lu and co-workers have demonstrated that by controlling the hydrogen bonding in the outer coordination sphere of a metalloprotein, Cu-azurin, the redox potential at the active site can be tuned over a range of 700 mV.⁵ Protein dynamics and stabilization of unusual conformations or oxidation states have also been observed to control reactivity in enzymes.^{1,4,6} An example of such control is the large-scale motion proposed for formate dehydrogenase when selenocysteine disassociates from molybdenum at the active site and moves 12 Å away, allowing formate to bind.^{7,8}

Hydrogenases are metalloenzymes that have received extensive interest due to their ability to efficiently interconvert protons and H₂, reactions that are important for utilizing intermittent energy sources such as solar and wind. Three active sites have been observed for hydrogenases: a single iron, an iron–nickel core, or two irons ([FeFe]).⁹ The active site of [FeFe]-hydrogenase, the focus of most biomimics in this area, is shown in Figure 1. While [FeFe]-hydrogenases can operate in both directions, they are typically biased toward H₂ production, operating at rates up to 20 000 s^{−1} with a 100 mV overpotential.^{9–11} The overpotential is the extra energy required to run the reaction over the thermodynamic potential,¹² and the low value observed for hydrogenases

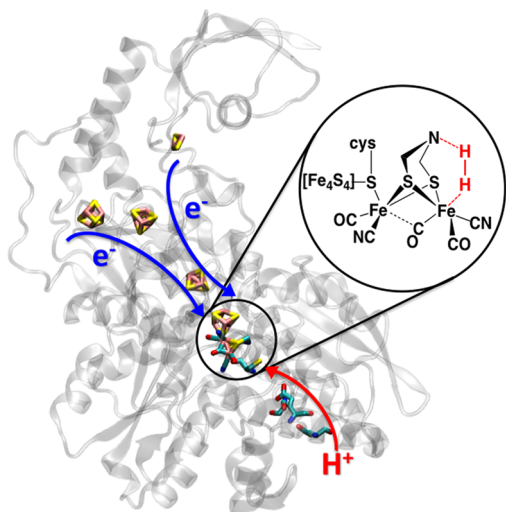


Figure 1. *Clostridium pasteurianum* [FeFe]-hydrogenase (PDB ID 3C8Y) with the electron channel (blue) and proton channel (red). The pendant amine works in concert with the active site to add H₂ (or bring protons together to release H₂).

allows reversible operation and is indicative of their high energy efficiency. An interesting structural feature of [FeFe]-hydrogenase is the presence of only a single connection of the active site to the peptide scaffold, through one cysteine, a feature that may suggest the importance of flexibility during catalysis.

While investigations devoted to the outer coordination sphere of hydrogenases have been sparse, the reported studies demonstrate its importance. For instance proton channels are needed to move protons to and out of the active site. Single-site mutations have identified a four-residue proton channel for [FeFe]-hydrogenase by nearly eliminating activity for each mutation, in both directions.^{13,14} Computational studies demonstrated that it was the residues themselves and not water surrounding the residues that were acting as the proton channel.^{15,16} The importance of residues not intimately associated with the active site has also been shown for [FeFe]-hydrogenases.^{14,17} As an example, the Léger group demonstrated that overpotential and catalytic bias is controlled not by the redox properties of the active site but by residues remote from the active site that control either H₂ release (H₂ production) or electron transfer (H₂ oxidation).¹⁷ These studies of the outer coordination sphere are providing critical information about how the scaffold controls activity and efficiency, but our understanding is still at a rudimentary level.

When considering the combination of rate and overpotential, hydrogenases still outperform any synthetic mimic. *Structural mimics*, or those complexes that try to reproduce the structure of the active site, have been studied extensively.¹⁸ Initial efforts have been made to attach peptides to the structural mimics via a “bottom-up” approach, that is, attaching a small peptide scaffold to the metal complex; however, with the complexes prepared thus far, no catalytic activity has been observed.^{19,20} “Top-down” approaches, or those attaching the metal complex to a protein with a well-defined structure, have resulted in functional catalysts.^{21,22} Cobalt–heme complexes have also been investigated and have activity for H₂ production in water but at high overpotentials.²³

Functional mimics of hydrogenase have focused on capturing essential features of the active site. In the crystal structure of [FeFe]-hydrogenase, a pendant amine is positioned in the second coordination sphere to bring two protons close enough to react and release as H₂ or to aid in binding H₂ for heterolytic cleavage (Figure 1). The use of a similarly positioned pendant amine in [Ni(P^R₂N^{R'}₂)₂]²⁺ molecular catalysts (Figure 2) (P₂N₂ = 1,5-diaza-3,7-diphosphacyclooctane) resulted in an increase in rate of over three orders of magnitude and lowered the overpotential for catalysis compared with analogous carbon-based analogues.²⁴ These complexes are active for either H₂ oxidation or H₂ production, tuned by modifying groups on phosphorus.^{24,25} The currently reported fastest rate for the

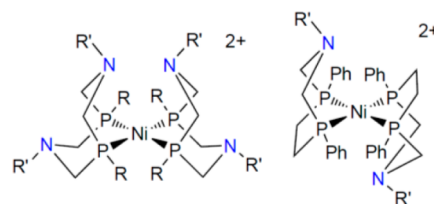


Figure 2. Functional mimics of [FeFe]-hydrogenase, [Ni(P^R₂N^{R'}₂)₂]²⁺ and [Ni(P^{Ph}₂N^{R'}₂)₂]²⁺, include a pendant amine seen in the active site and have been used for studies of the outer coordination sphere.

functional mimics is observed for $[\text{Ni}(\text{P}^{\text{Ph}}_2\text{N}^{\text{C}_6\text{H}_4\text{OH}}_2)_2]^{2+}$ at $170\,000\text{ s}^{-1}$ at an overpotential of 475 mV in a 1:1 mixture of acetonitrile and water,²⁶ while the lowest overpotential (50 mV) is observed for $[\text{Ni}(\text{P}^{\text{Ph}}_2\text{N}^{\text{Bn}}_2)_2]^{2+}$, operating at 4 s^{-1} in acetonitrile.²⁷ For H_2 oxidation, the fastest reported rate is 60 s^{-1} for $[\text{Ni}(\text{P}^{\text{Cy}}_2\text{N}^{\text{tBu}}_2)_2]^{2+}$ in acetonitrile with a reported (unoptimized) overpotential of 500 mV.²⁸ These results show impressive advancements in achieving fast rates and low overpotentials but also demonstrate the challenge of achieving both in the same complex, challenges that may be overcome by the addition of outer coordination sphere features from the enzyme.

In this Account, we focus on effects of an outer coordination sphere on both the $[\text{Ni}(\text{P}^{\text{R}}_2\text{N}^{\text{R}'}_2)_2]^{2+}$ and $[\text{Ni}(\text{P}^{\text{R}}_2\text{N}^{\text{R}'}_2)]^{2+}$ ($\text{P}_2\text{N} = 1\text{-aza-3,6-diphosphacycloheptane}$) functional mimics. The $[\text{Ni}(\text{P}^{\text{R}}_2\text{N}^{\text{R}'}_2)]^{2+}$ complexes are well-studied, including thermodynamic properties, proton movement, substituent effects, and electronic properties, and have high activities, making them excellent core complexes on which an outer coordination sphere can be built and tested. This “bottom-up” approach allows the introduction and testing of features of the outer coordination sphere individually (for instance, the addition of a single carboxylic acid group), providing the ability to evaluate each feature mechanistically. This provides an advantage over evaluating effects of single site mutations in the enzyme, where identifying and decoupling the changes of modified function due to mutations (structure, dynamics, hydrogen bonding, etc.) can be a challenge. Our focus has been to evaluate the impact of single amino acids or functional groups first and then extend this knowledge by adding a structured outer coordination sphere that can introduce the precise positioning reminiscent of enzymes. Ultimately, this should allow us to understand precisely how different amino acids (alone or within the context of a peptide) influence and control catalytic activity. This will arise from an in-depth understanding of how the outer coordination sphere functions in molecular catalysts and, by extension, the role of the protein scaffold used by enzymes.

■ H₂ OXIDATION

For the $[\text{Ni}(\text{P}^{\text{R}}_2\text{N}^{\text{R}'}_2)_2]^{2+}$ mimics, the H_2 oxidation complexes are less well-studied compared with the H_2 production complexes, and investigations of the outer coordination sphere began by attaching simple functional groups and amino acids. The focus of this work was appending proton channels to facilitate proton movement from the active site, analogous to enzyme function, with the ultimate goal of understanding the mechanistic details of proton channels and their influence on catalytic properties.

Functional Groups in the Outer Coordination Sphere

To test whether functional groups in the outer coordination sphere can modulate catalytic activity, simple two-relay proton channels were created by replacing the benzyl (Bn) in the active H_2 oxidation catalyst, $[\text{Ni}(\text{P}^{\text{Cy}}_2\text{N}^{\text{Bn}}_2)_2]^{2+}$, with a pyridazyl (Pyz) group, $[\text{Ni}(\text{P}^{\text{Cy}}_2\text{N}^{\text{Pyz}}_2)_2]^{2+}$ (Figure 3).²⁹ Previous studies had shown that water could be used as a base for H_2 oxidation of $[\text{Ni}(\text{P}^{\text{Cy}}_2\text{N}^{\text{Bn}}_2)_2]^{2+}$,³⁰ but this resulted in an overpotential of 900 mV. By introduction of pyridazine groups, the overpotential using water as a base was lowered by 300 mV (Figure 3). This was attributed to enhanced proton movement from the active site via the pyridazines based on low temperature NMR and room temperature electrochemistry studies. The pyridazine

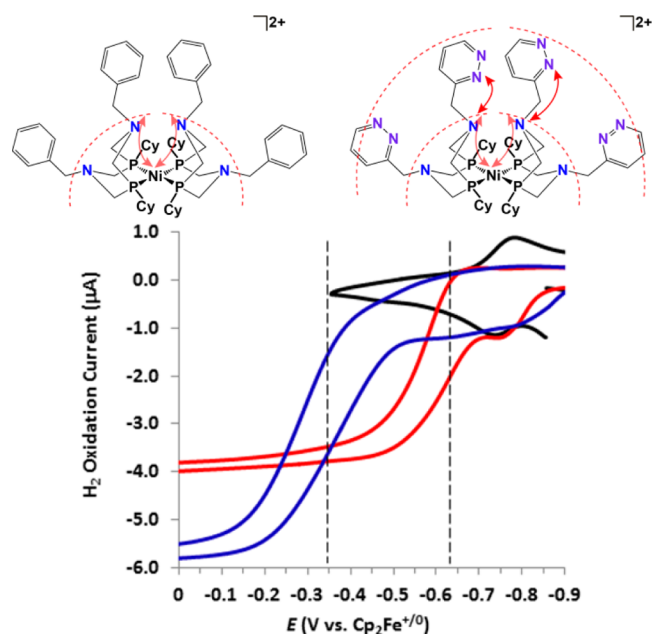


Figure 3. Cyclic voltammograms in 5M H₂O in acetonitrile of: $[\text{Ni}(\text{P}^{\text{Cy}}_2\text{N}^{\text{Pyz}}_2)_2]^{2+}$ under N₂ (black) and under H₂ (red) and $[\text{Ni}(\text{P}^{\text{Cy}}_2\text{N}^{\text{Bn}}_2)_2]^{2+}$ under H₂, showing activity for H₂ oxidation, as well as the drop in overpotential for catalysis by 300 mV for $[\text{Ni}(\text{P}^{\text{Cy}}_2\text{N}^{\text{Pyz}}_2)_2]^{2+}$. Vertical lines indicate the $E_{\text{cat}/2}$ for each complex.²⁹ Adapted with permission from ref 29. Copyright 2014 the Royal Society of Chemistry.

groups also resulted in bypassing the endo–endo isomer, a thermodynamic well in the catalytic cycle (Figure 4).

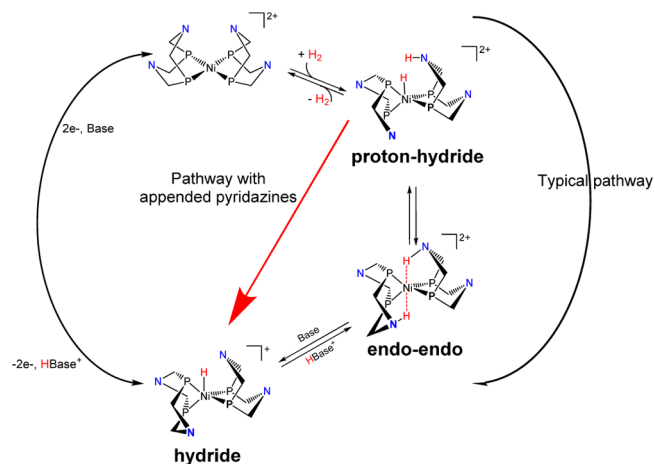


Figure 4. Pyridazine groups in the outer coordination sphere of $[\text{Ni}(\text{P}^{\text{Cy}}_2\text{N}^{\text{Pyz}}_2)_2]^{2+}$ enable bypassing a thermodynamic well in the catalytic cycle.²⁹ Adapted with permission from ref 29. Copyright 2014 the Royal Society of Chemistry.

Unfortunately, the rate of H_2 oxidation was also lower, likely due to weak binding of pyridazine to Ni. However, this provided a demonstration of the ability of the outer coordination sphere to directly impact the energy efficiency (overpotential) of catalysis. In a second system with ether substituents ($\text{CH}_2\text{CH}_2\text{OCH}_3$) replacing the pyridazine groups, a 150 mV drop in overpotential was observed compared with $[\text{Ni}(\text{P}^{\text{Cy}}_2\text{N}^{\text{Bn}}_2)_2]^{2+}$, demonstrating the general effect of an additional proton relay.³¹

Amino Acid Outer Coordination Sphere

To create a more direct mimic of enzymes, we incorporated amino acids into the outer coordination sphere of H₂ oxidation catalysts. While single amino acids typically have limited ability to stabilize structure, they do offer the broad range of functional groups, chirality, and pK_a's that are found in enzymes.

Initial attempts to incorporate an amino acid based outer coordination sphere built upon the active [Ni(P^{Cy}₂N^{Bn})₂]²⁺ complex³⁰ by appending alanine ester or phenylalanine ester to the *para*-position of the benzyl ring via a carboxylic acid ([Ni(P^{Cy}₂N^{Bn-COOH})₂]²⁺).³² Both complexes were active for H₂ oxidation but were slower than [Ni(P^{Cy}₂N^{Bn})₂]²⁺, due to the reduced pK_a of the pendant amine upon the addition of the electron withdrawing carboxylate group. Besides the electron withdrawing effect, there was no clear impact of the outer coordination sphere, possibly the result of the bulky benzyl groups blocking the amino acids from the active site. The crystal structure of the complex containing carboxylic acid esters shows the steric congestion (Figure 5). While these complexes did provide a platform upon which peptides could be attached, the results suggested that a different approach would be more fruitful.

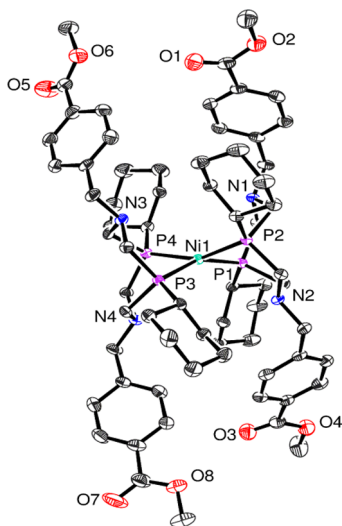


Figure 5. Crystal structure of [Ni(P₂CyN₂^{Bn-COOMe})₂]²⁺ has a similar active site structure as [Ni(P^{Cy}₂N^{Bn})₂]²⁺. The addition of the ester reduced activity due to electron withdrawing effects. Attaching amino acids to the carboxylic acid did not further impact catalytic activity, possibly due to the steric bulk of the benzyl rings blocking access to the active site. Ni, green; N, blue; P, purple; O, red; C, black. Reproduced from ref 32. Copyright 2012 American Chemical Society.

To improve the possibility of interactions between the side chain of the amino acid and the active site, the amine of the amino acid glycine was incorporated directly into the P^{Cy}₂N^{R'}₂ macrocycle, resulting in [Ni^{II}(P^{Cy}₂N^{Gly})₂]⁴⁺ (the 4+ charge is due to protonation under acidic conditions).³³ Important differences between this complex and other [Ni^{II}(P^{Cy}₂N^{R'})₂]²⁺ derivatives were observed. First, [Ni^{II}(P^{Cy}₂N^{Gly})₂]⁴⁺ is completely soluble in water, while other derivatives are studied primarily in acetonitrile. The second difference was found in the cyclic voltammetry: with other derivatives in acetonitrile, the Ni^{II/I} and Ni^{I/0} couples are well separated, by as much as 550 mV.^{30,32} For [Ni^{II}(P^{Cy}₂N^{Gly})₂]⁴⁺, the two waves were found to be overlapping in methanol or water (the

[Ni⁰(P^{Cy}₂N^{Gly})₂]²⁺ has limited solubility in acetonitrile, but the I/0 wave also appears to overlap the II/I wave), the importance of which is discussed below.

In water, the resulting complex was active for H₂ oxidation from pH = 0–9, with the fastest rates (33 s⁻¹) observed at pH = 0.7 (Figure 6), conditions relevant to those of proton exchange membrane (PEM) fuel cells. Past observations have suggested that matching the pK_a of the pendant amine to the base in solution enhances the observed rates.^{26,27} Based on those observations, the fastest rates would be expected at pK_a ≈ 7, the measured pK_a of the pendant amine. There is a local maximum at this pK_a, but rates are still three to four times slower than at the optimal pK_a.³³ One explanation for the fast rates at low pH for this complex may be due to catalysis occurring through the triply protonated species (i.e., three pendant amines protonated instead of only two), a mechanism that is being investigated.

This complex also operated at the low overpotential of 150 mV for H₂ oxidation, an energy efficiency approaching that of the enzyme (~100 mV).³³ The overlapping II/I and I/0 waves noted above and their changing potential as a function of pH, while remaining overlapped, are suggestive of fast proton transfer coupled with electron transfer. Infrared studies of the COOH stretch confirmed proton transfer between the pendant amines and the carboxylic acid groups, demonstrating that this simple outer coordination sphere was acting as a two-relay proton channel. The low overpotential may be a result of rapid proton movement, and control complexes that can test this theory are currently being investigated. This complex was also active for H₂ production (Figure 6, red data), but electrochemical studies showed that the active form of the H₂ production catalyst is immobilized on the electrode surface, resulting in high overpotentials (up to 750 mV).

A related second complex was prepared, replacing glycine with arginine ([Ni^{II}(P^{Cy}₂N^{Arg})₂]⁸⁺, Figure 7).³⁴ This placed guanidinium groups in the outer coordination sphere, with the intention of adding a third relay to extend our proton channel; their actual function is much more interesting. The resulting complex was six times faster for H₂ oxidation than the glycine complex (210 s⁻¹ vs 33 s⁻¹) at 1 atm H₂ with an overpotential of 180 mV. At high pressure (133 atm H₂), it operated at 144 000 s⁻¹ but at the expense of a higher overpotential (480 mV).

The complex showed a linear dependence on H₂ pressure, suggesting that the enhanced rates compared with glycine were due to faster H₂ addition, not faster proton movement. Proteins often use arginine–arginine interactions to provide structural stability through a quasi-aromatic interaction,³⁵ so we tested our complex to see whether that might have a role in [Ni^{II}(P^{Cy}₂N^{Arg})₂]⁸⁺. Electrochemical studies demonstrated that conditions that disrupted the arginine–arginine interaction also significantly slowed catalysis, providing evidence in favor of this interaction and discounting the hypothesis that the charge alone (8+ at low pH) is responsible for the fast rates.³⁴ H₂ addition and subsequent heterolytic cleavage may be sensitive to the Ni...N distance, and the observed results are consistent with arginine–arginine interactions improving this distance.³⁴ Structural studies are ongoing to provide direct evidence of this interaction.

Fast proton movement was established for [Ni^{II}(P^{Cy}₂N^{Arg})₂]⁸⁺ based on the high catalytic rates as well as the pH-dependent overpotentials. At low turnover frequencies, under conditions where the carboxylates are protonated (pH = 1–3), the overpotentials are independent

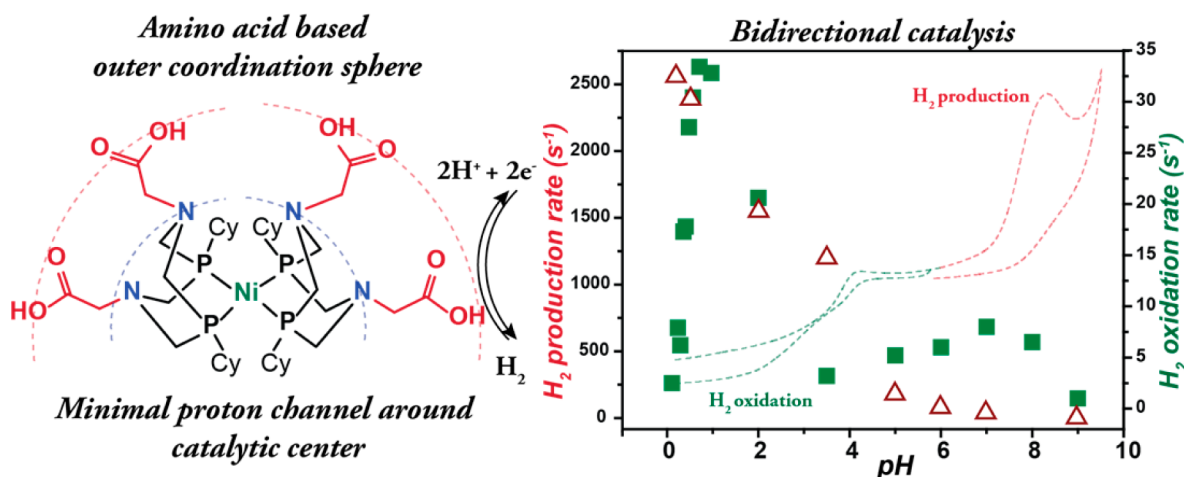


Figure 6. The amine of glycine was incorporated directly into $[\text{Ni}^{\text{II}}(\text{P}^{\text{Cy}_2\text{N}^{\text{Gly}}_2)_2]^{4+}$ (left). The resulting complex was observed to transfer protons rapidly between the pendant amine and the COOH, was water-soluble, and (right) was functional for both H_2 production (red triangles) and oxidation (green squares). Adapted from ref 33. Copyright 2013 American Chemical Society.

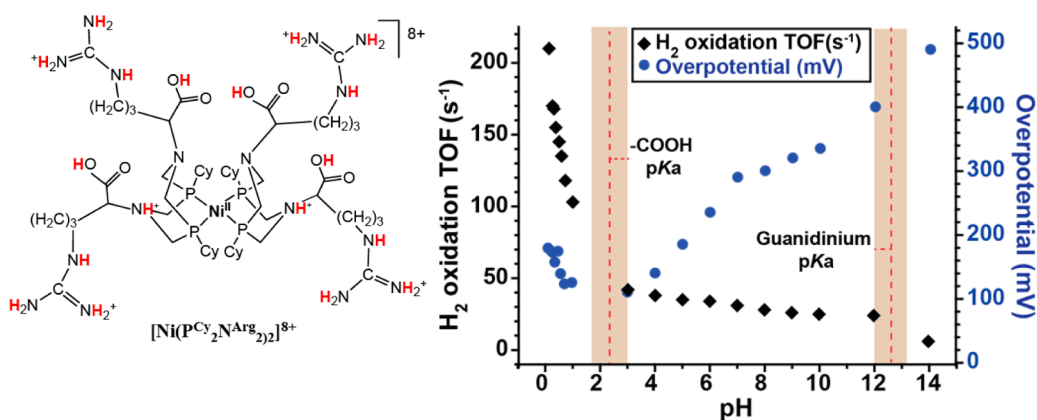


Figure 7. $[\text{Ni}^{\text{II}}(\text{P}^{\text{Cy}_2\text{N}^{\text{Arg}}_2)_2]^{8+}$ is an active H_2 oxidation catalyst at all pH values, with the fastest rates at low pH, conditions most relevant for fuel cells. Overpotentials also vary as a function of pH, demonstrating a dependence on proton or electron transfer or both at high rates. Adapted from ref 34. Copyright 2014 John Wiley and Sons.

of pH, as expected for a system under equilibrium control.³⁴ At higher pH, the COOH groups are deprotonated and higher overpotentials are observed, thought to be due to the COO^- group hindering proton transfer. Faster rates, observed at lower pH or higher pressure, also result in higher overpotentials (Figure 7). This suggests that either proton or electron movement has deviated from equilibrium conditions, resulting in an increased overpotential, and directly connects proton or electron movement to overpotentials. Despite the high overpotentials at the fastest rates, the observed rates at high pressure are 3 orders of magnitude faster than any reported synthetic H_2 oxidation complex, providing the opportunity to probe more in-depth questions regarding the rates of electron and proton transfer and their effects on both rate and overpotential.

■ H_2 PRODUCTION

H_2 production complexes in the $[\text{Ni}(\text{P}^{\text{Ph}}_2\text{N}^{\text{Ph}}_x)_2]^{2+}$ family are more well-studied and more stable than H_2 oxidation complexes, and evidence of outer coordination sphere interactions was observed based on a large role of water and ionic liquids in enhancing rates.^{36,37} Therefore, studies with

these mimics began with dipeptides and have advanced to studies of structured peptides.

Amino Acid Outer Coordination Sphere

The first studies of amino acid based complexes for H_2 production focused on controlling the environment around the active site such as the hydrophobicity, hydrophilicity, and dielectric by introducing amino acids with different functional groups. These complexes were synthesized by replacing the nitrogen bound phenyl (Ph) in the well-understood $[\text{Ni}(\text{P}^{\text{Ph}}_2\text{N}^{\text{Ph}}_2)_2]^{2+}$ with the non-natural amino acid 4-aminophenyl propionic acid (NNA), giving $[\text{Ni}(\text{P}^{\text{Ph}}_2\text{N}^{\text{NNA}}_2)_2]^{2+}$.^{38–40} Three complexes were prepared from this core complex, including the acid, ester, and amide forms ($\text{R}'' = \text{OH}$, OMe and NH_2 in Figure 8). To create a dipeptide containing complex ($[\text{Ni}(\text{P}^{\text{Ph}}_2\text{N}^{\text{NNA-amino-acid}}_2)_2]^{2+}$), the acid form was coupled to a second amino acid or amino acid ester, including alanine, alanine ethyl ester, serine methyl ester, phenylalanine methyl ester, tyrosine methyl ester, glutamic acid, glutamic acid ester, aspartic acid, aspartic acid ester, lysine, and lysine ester (Figure 8).

Rate enhancements were observed for nearly all of the amino acid and dipeptide complexes. The rates of the resulting complexes were compared as a function of amino acid side

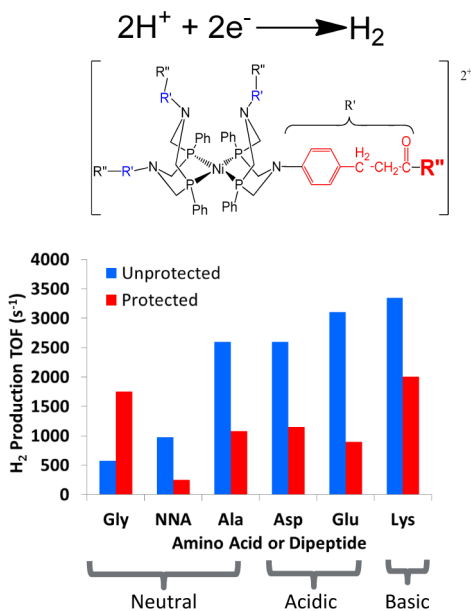


Figure 8. Dipeptides created by coupling the non-natural amino acid linker ($R' = \text{NNA}$) with a variety of amino acids ($R'' = \text{Gly, Ala, Asp, Glu, Lys}$) yield an order of magnitude difference in rates of H_2 production, as much as five times faster than the $[\text{Ni}(\text{P}^{\text{Ph}}_2\text{N}^{\text{Ph}}_2)_2]^{2+}$ parent complex.^{38–40}

chain and whether or not the side chain or backbone was protected, and increased in the following order: basic > acidic > nonpolar \approx polar (Figure 8).^{38–40} The rate enhancement for the complexes containing nonpolar or polar amino acids ($\sim 10\%$) was attributed to the amide group, based on the lack of any other observed differences for this set of complexes, and based upon a similar rate observed for the amide terminated complex.⁴⁰ Complexes with acidic or basic side chain or backbone moieties resulted in rate enhancements of up to five times compared with the unmodified parent complex ($[\text{Ni}(\text{P}^{\text{Ph}}_2\text{N}^{\text{Ph}}_2)_2]^{2+}$; 720 s^{-1}).³⁶ Protecting the amino acid backbone or side chain reduced the rate in nearly all cases (glycine being the exception).^{38,39} Replica exchange molecular dynamics (REMD) studies suggested that faster rates were a result of basic or acidic functional groups concentrating water (water has been observed to enhance the rate of catalysis by 1.5–50-fold)²⁵ and possibly protons, around the active site, a mechanism often employed in enzymes.⁴⁰

Perhaps the most significant result obtained by REMD was revealing the highly flexible nature of dipeptides within the complex (Figure 9).⁴⁰ The extensive phase space that the dipeptide ligands cover eliminates the possibility of the precise positioning achieved by enzymes and necessitates a larger scaffold or stabilizing mechanism to limit and control the dynamics.

Peptide/Protein Based Outer Coordination Sphere (“Bottom-Up”)

Due to the structural flexibility observed in the dipeptide containing complexes, a larger peptide with stable structure was desired to achieve the limited range of motion in enzymes, which stabilizes the positioning of functional groups around the active site. Building upon the success of the amino acid and dipeptide catalysts, we prepared a H_2 production complex with a structured peptide in the outer coordination sphere ($[\text{Ni}(\text{P}^{\text{Ph}}_2\text{N}^{\text{NNA-hairpin}})_2]^{2+}$; Figure 10).⁴¹ In this case the

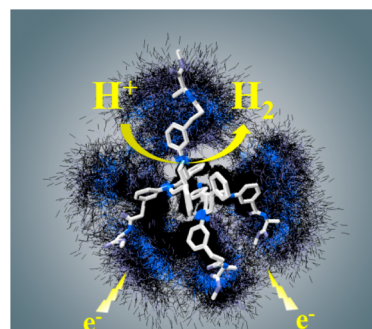


Figure 9. Dipeptides in the outer coordination sphere of $\text{Ni}(\text{P}^{\text{Ph}}_2\text{N}^{\text{NNA-amino-acid}}_2)_2$ complexes enhance the rate by as much as five times but are too flexible (shown here by overlapping REMD trajectories) to position functional groups in a single location.⁴⁰

$[\text{Ni}(\text{P}^{\text{Ph}}_2\text{N}^{\text{R}'}_2)_2]^{2+}$ core (right side of Figure 2) was used instead of the $[\text{Ni}(\text{P}^{\text{R}'}_2\text{N}^{\text{R}'}_2)_2]^{2+}$ core (left side of Figure 2) to avoid problematic synthetic challenges created by trying to attach four peptides onto one complex using solid state synthetic methods. A β -hairpin structure (WlppRWtGPR)⁴² was chosen due to its high stability to temperature, its extensive structural characterization, and its flexible primary structure outside of a few residues (indicated in bold). Importantly, the turn forces the peptide to come back toward the metal allowing maximum interaction of the peptide with the complex, a feature harder to achieve with helical peptides unless strong peptide–peptide interactions can be realized.⁴³ A concerted effort was made to understand both structure and function, so that ultimately a correlation between the two could be made for this synthetic enzyme.

The structure of the hairpin for $\text{Ni}(\text{P}^{\text{Ph}}_2\text{N}^{\text{NNA-hairpin}})_2^{2+}$ was confirmed with 1D and 2D NMR, as well as circular dichroism, to be 70–80% β -hairpin. Unfortunately, NOEs from the hairpin to the propionic acid linker, which would position the orientation of the peptide with respect to the active site, were not observed. To provide insight into relative orientation, we performed Förster resonance energy transfer (FRET) measurements to determine the distance from the two tryptophan groups to the Ni. These experiments were consistent with two distinct distances, shown by molecular dynamics simulations to be the distances to either tryptophan, although the significant flexibility of the linker allowed either W1 or W6 to be closer to the metal (Figure 10). MD results are most consistent with the two distinct distances corresponding to the up–down configuration of the ligands, as shown (as opposed to the amines being on the same side, “up–up”). The complex is an active H_2 production catalyst ($\sim 100\,000 \text{ s}^{-1}$), and the peptide enables it to operate at twice the rate of the non-natural amino acid substituted parent complex. However, despite the longer chain and the structural stability of the hairpins, there is still significant hinge-like flexibility around the linker (Figure 11), limiting the desired enzyme-inspired positioning and making it difficult to correlate any particular functional group with enhanced rates. Despite this, the preparation of this active, structured complex was an important advancement in demonstrating both the structure and function of a peptide-based H_2 production complex. Further studies with a benzoic acid linker instead of a propionic acid linker were prepared in an attempt to limit the mobility of the hairpin relative to the core. While active for H_2 production, the benzoic acid–hairpin complexes restricted motion significantly based on ^{31}P NMR,

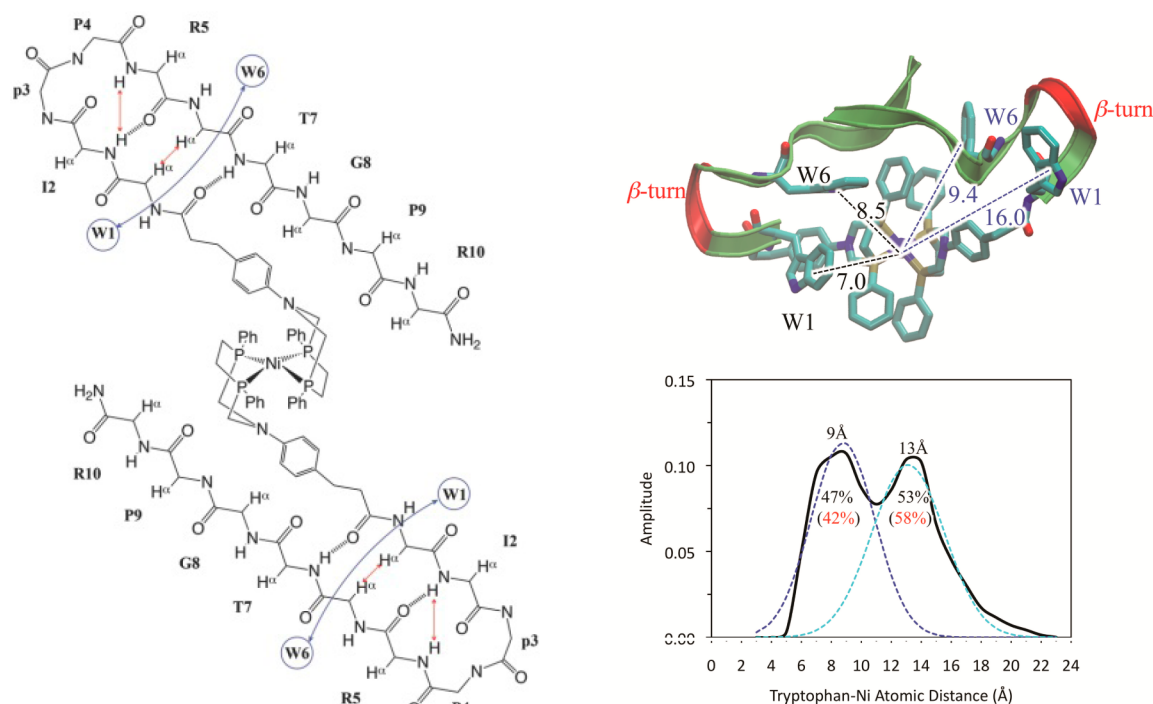


Figure 10. $[\text{Ni}(\text{P}^{\text{Ph}}_2\text{N}^{\text{NNA-hairpin}})_2]^{2+}$ complex is an active H_2 production catalyst. FRET measurements were used to identify two populations of structures (red numbers) and MD (black numbers) consistent with the up–down confirmation shown above.³⁸ Reproduced with permission from ref 41. Copyright 2014 John Wiley and Sons.

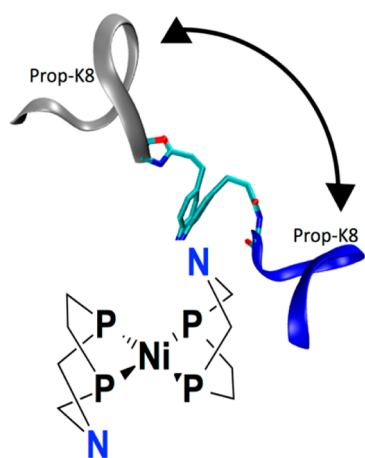


Figure 11. Two of the peptide conformations relative to the core of $\text{Ni}(\text{P}^{\text{Ph}}_2\text{N}^{\text{NNA-hairpin}})_2^{2+}$ due to the hinge-like motion of the linker (only one peptide is shown for clarity). While motion is more restricted than for single amino acids or dipeptides, limiting mobility for “bottom-up” synthetic mimics is still needed to achieve the positioning of enzymes.

and resulted in multiple interchanging waves in the cyclic voltammetry (unpublished results). This behavior prevented us from quantitating the data and highlights the sensitivity of these complexes to fairly subtle changes in structure and flexibility, reminiscent of enzymatic behavior.

■ “TOP-DOWN” OUTER COORDINATION SPHERE

Using a “top-down” approach,⁴⁴ starting with a well-structured protein to which a metal complex is attached, Silver et al.⁴⁵ prepared $[\text{Ni}(\text{P}^{\text{Ph}}_2\text{N}^{\text{Ph}})_2]^{2+}$ assembled with either photosystem I (PSI) or apoflavodoxin (ApoFld), one of the naturally occurring electron acceptors for PSI. Both proteins showed

photocatalytic activity in water, with the Ni–ApoFld:PSI complex being approximately two times more active than the Ni–PSI alone ($\text{TOF} = 1.25 \text{ mol H}_2 (\text{mol PSI})^{-1} \text{ s}^{-1}$).⁴⁵ This suggests either a more specific binding of $[\text{Ni}(\text{P}^{\text{Ph}}_2\text{N}^{\text{Ph}})_2]^{2+}$ to ApoFld or a stabilization of the metal complex when Ni–ApoFld binds to PSI. Detailed structural characterization that could provide insight into the interaction between the metal complex and the protein is lacking. However, if structural information were determined, this system could be a very elegant method with which to introduce a well-structured and likely tunable outer coordination sphere, providing the ability to understand structure–function relationships that may enhance catalytic activity. A similar approach was taken by Hayashi’s group²² and Artero’s group²¹ using the diiron structural mimic, demonstrating its generality. These “top-down” approaches demonstrate promise in allowing us to probe the role of a large structured protein on catalytic activity, as soon as structure–function relationships can be established.

■ SUMMARY AND PERSPECTIVE

The current understanding of enzymes suggests that features beyond the active site of the enzyme can dramatically influence catalytic activity and efficiency. Understanding how amino acids and peptides influence catalytic function will reveal the role of the outer coordination sphere in these catalysts and may lead to new insights in how protein matrices influence the active sites of enzymes. While this area is still in the early stages of development, incorporating enzyme-inspired functionality onto molecular catalysts is starting to provide enhancements in rates, lower overpotentials, and fast proton movement and, even more importantly, general principles that may ultimately be used for catalyst design. For instance, charged groups are capable of concentrating substrate, in a manner reminiscent of proteins.^{38–40} Functional groups positioned appropriately can

shuttle protons,^{29,31,33,34} and structural features, such as guanidinium–guanidinium interactions, can control the rate of substrate addition by controlling the structure of the active site.³⁴ A common theme has been the remarkable changes observed with a relatively simple outer coordination sphere that is remote from the active site. For the “bottom-up” approach, limiting structural flexibility of the peptide scaffold relative to the core complex remains a challenge. However, restricting the flexibility drastically altered the electrochemical behavior, emphasizing the subtle sensitivity of structure and function; both small scale and large scale dynamic freedom is needed, and learning to control these motions in molecular catalysts is an important goal. “Top-down” approaches face the major hurdle of obtaining structural data to allow structure–function comparisons, but the advantage is that the structure is stable, so once the location of the metal complex is determined, single site mutants should provide a wealth of understanding. This approach also suffers from the large size of the resulting complex, and from limited knowledge about the essential features of the protein scaffold. This leads to the larger outstanding question: how much scaffold is needed to account for the outer coordination sphere features? The assumption from many proponents who favor including a scaffold is that it does not need to be as large as a protein, but it does need to be large enough to have well-defined structure. Our observations from complexes with amino acids or dipeptides demonstrate the influence of this minimal outer coordination sphere on proton movement and structure to provide significant differences in rate and overpotential. While it is not a solved problem, it does result in an adjustment of how we consider structure in enzymes vs molecular catalysts and points to the need to constantly evaluate how we implement features from nature for technological applications. Ultimately, it is likely that an intermediate construct (i.e., not a full protein, but larger than 1–10 amino acids) will provide the optimal compromise between size and functionality. Extending our focus from direct to conceptual mimics of proteins such as polymers, nanomaterials, and inorganic scaffolds may provide the most robust material for practical applications. Meanwhile, the knowledge we are gaining from understanding the role of amino acids, peptides, and proteins attached to our metal complexes is invaluable in developing fundamental design principles of the function of the outer coordination sphere.

AUTHOR INFORMATION

Corresponding Author

*E-mail: wendy.shaw@pnnl.gov.

Notes

The authors declare no competing financial interest.

Biographies

Bojana Ginovska-Pangovksa is a Scientist at PNNL. She received her M.Sc. degree from Washington State University. Her research interests include theoretical approaches to understanding reaction mechanisms in metal and nonmetal based molecular catalysts for energy applications.

Aarnab Dutta joined PNNL as a postdoctoral associate in 2012 after receiving his Ph.D. in Chemistry from Arizona State University. He is currently interested in developing bioinspired catalysts for H₂ oxidation and production using a “bottom-up” approach.

Matthew L. Reback was a postdoctoral associate at PNNL from 2010 to 2014 and is currently a postdoctoral associate at CEA, Grenoble, France. His research interests include the relationship between the outer coordination sphere and the active site of catalysts for renewable energies and the design of organometallic complexes for anticancer agents.

Since receiving his Ph.D. from UC Davis in 1987, **John Linehan** has spent his career at PNNL investigating energy related catalysis from direct coal liquefaction to hydroformylation in supercritical fluids to using first row transition metal catalysts for CO₂ hydrogenation, using thermodynamic properties for catalyst design and *in operando* spectroscopies (NMR, FTIR, XAFS) to interrogate catalytic mechanisms.

Wendy J. Shaw is a Senior Research Scientist at PNNL. She received her Ph.D. from the University of Washington. Her research interests emphasize learning from nature and include understanding the contribution of an enzyme like outer coordination sphere on molecular catalysts with relevance for renewable energies and understanding protein–surface interactions for biomineralization systems.

ACKNOWLEDGMENTS

This Account reviews previously published work supported by the Office of Science Early Career Research Program through the USDOE, Basic Energy Sciences (BES); USDOE BES, Chemical Sciences, Geoscience and Biosciences; USDOE BES, Physical Biosciences; the Center for Molecular Electrocatalysis, an Energy Frontier Research Center funded by the USDOE, Office of Science, Office of BES. Part of the research was conducted at the W.R. Wiley Environmental Molecular Sciences Laboratory, a national scientific user facility sponsored by USDOE's Office of Biological and Environmental Research program located at Pacific Northwest National Laboratory (PNNL). PNNL is operated by Battelle for the USDOE. We thank Dr. Charles Weiss for assistance with the Conspectus graphic.

REFERENCES

- (1) Ragsdale, S. W. Metals and their scaffolds to promote difficult enzymatic reactions. *Chem. Rev.* **2006**, *106*, 3317–3337.
- (2) Creighton, T. E. *Proteins: Structures and Molecular Properties*, 2nd ed.; W.H. Freeman and Company: New York, 1993.
- (3) Karlin, S.; Zhu, Z. Y.; Karlin, K. D. The extended environment of mononuclear metal centers in protein structures. *Proc. Natl. Acad. Sci. U.S.A.* **1997**, *94*, 14225–14230.
- (4) Gora, A.; Brezovsky, J.; Damborsky, J. Gates of enzymes. *Chem. Rev.* **2013**, *113*, 5871–5923.
- (5) Marshall, N. M.; Garner, D. K.; Wilson, T. D.; Gao, Y.-G.; Robinson, H.; Nilges, M. J.; Lu, Y. Rationally tuning the reduction potential of a single cupredoxin beyond the natural range. *Nature* **2009**, *462*, 113–116.
- (6) Lee, J.; Goodey, N. M. Catalytic contributions from remote regions of enzyme structure. *Chem. Rev.* **2011**, *111*, 7595–7624.
- (7) Boyington, J. C.; Gladyshev, V. N.; Khangulov, S. V.; Stadtman, T. C.; Sun, P. D. Crystal structure of formate dehydrogenase H: Catalysis involving Mo, molybdopterin, selenocysteine, and an Fe₄S₄ cluster. *Science* **1997**, *275*, 1305–1308.
- (8) Raaijmakers, H. C.; Romao, M. J. Formate-reduced *E. coli* formate dehydrogenase H: The reinterpretation of the crystal structure suggests a new reaction mechanism. *J. Biol. Inorg. Chem.* **2006**, *11*, 849–854.
- (9) Fontecilla-Camps, J. C.; Volbeda, A.; Cavazza, C.; Nicolet, Y. Structure/function relationships of [NiFe]- and [FeFe]-hydrogenases. *Chem. Rev.* **2007**, *107*, 4273–4303.

- (10) Madden, C.; Vaughn, M. D.; Diez-Perez, I.; Brown, K. A.; King, P. W.; Gust, D.; Moore, A. L.; Moore, T. A. Catalytic turnover of [FeFe]-hydrogenase based on single-molecule imaging. *J. Am. Chem. Soc.* **2012**, *134*, 1577–1582.
- (11) Vincent, K. A.; Parkin, A.; Armstrong, F. A. Investigating and exploiting the electrocatalytic properties of hydrogenases. *Chem. Rev.* **2007**, *107*, 4366–4413.
- (12) Saveant, J.-M. Molecular catalysis of electrochemical reactions. Mechanistic aspects. *Chem. Rev.* **2008**, *108*, 2348–2378.
- (13) Cornish, A. J.; Gartner, K.; Yang, H.; Peters, J. W.; Hegg, E. L. Mechanism of proton transfer in [FeFe]-hydrogenase from *Clostridium pasteurianum*. *J. Biol. Chem.* **2011**, *286*, 38341–38347.
- (14) Knorz, P.; Silakov, A.; Foster, C. E.; Armstrong, F. A.; Lubitz, W.; Happe, T. Importance of the protein framework for catalytic activity of [FeFe]-hydrogenases. *J. Biol. Chem.* **2012**, *287*, 1489–1499.
- (15) Ginovska-Pangovska, B.; Ho, M.-H.; Linehan, J. C.; Cheng, Y.; Dupuis, M.; Raugei, S.; Shaw, W. J. Molecular dynamics study of the proposed proton transport pathways in [FeFe]-hydrogenase. *Biochim. Biophys. Acta, Bioenerg.* **2014**, *1837*, 131–138.
- (16) Long, H.; King, P. W.; Chang, C. H. Proton transport in *Clostridium pasteurianum* [FeFe]-hydrogenase I: A computational study. *J. Phys. Chem. B* **2014**, *118*, 890–900.
- (17) Hamdan, A. A.; Dementin, S.; Liebgott, P.-P.; Gutierrez-Sanz, O.; Richaud, P.; Lacey, A. L. D.; Rousset, M.; Bertrand, P.; Cournac, L.; Leger, C. Understanding and tuning the catalytic bias of hydrogenase. *J. Am. Chem. Soc.* **2012**, *134*, 8368–8371.
- (18) Gloaguen, F.; Rauchfuss, T. B. Small molecule mimics of hydrogenases: Hydrides and redox. *Chem. Soc. Rev.* **2009**, *38*, 100–108.
- (19) Jones, A. K.; Lichtenstein, B. R.; Dutta, A.; Gordon, G.; Dutton, P. L. Synthetic hydrogenases: Incorporation of an iron carbonyl thiolate into a designed peptide. *J. Am. Chem. Soc.* **2007**, *129*, 14844–14845.
- (20) Roy, S.; Shinde, S.; Hamilton, G. A.; Hartnett, H. E.; Jones, A. K. Artificial [FeFe]-hydrogenase: On resin modification of an amino acid to anchor a hexacarbonyldiiron cluster in a peptide framework. *Eur. J. Inorg. Chem.* **2011**, 1050–1055.
- (21) Berggren, G.; Adamska, A.; Lambert, C.; Simmons, T. R.; Esselborn, J.; Atta, M.; Bambarelli, S.; Mouesca, J.-M.; Reijerse, E.; Lubitz, W.; Happe, T.; Artero, V.; Fontecave, M. Bimimetic assembly and activation of [FeFe]-hydrogenases. *Nature* **2013**, *499*, 66–69.
- (22) Sano, Y.; Onoda, A.; Hayashi, T. Photocatalytic hydrogen evolution by a diiron hydrogenase model based on a peptide fragment of cytochrome c_{556} with an attached diiron carbonyl cluster and an attached ruthenium photosensitizer. *J. Inorg. Biochem.* **2012**, *108*, 159–162.
- (23) Kleingardner, J. G.; Kandemir, B.; Bren, K. L. Hydrogen evolution from neutral water under aerobic conditions catalyzed by cobalt microperoxidase-11. *J. Am. Chem. Soc.* **2013**, *136*, 4–7.
- (24) Rakowski DuBois, M.; DuBois, D. L. The roles of the first and second coordination spheres in the design of molecular catalysts for H_2 production and oxidation. *Chem. Soc. Rev.* **2009**, *38*, 62–72.
- (25) Shaw, W. J.; Helm, M. L.; DuBois, D. L. A modular, energy-based approach to the development of nickel containing molecular electrocatalysts for hydrogen production and oxidation. *Biochim. Biophys. Acta, Bioenerg.* **2013**, *1827*, 1123–1139.
- (26) Hoffert, W. A.; Roberts, J. A. S.; Bullock, R. M.; Helm, M. L. Production of H_2 at fast rates using a nickel electrocatalyst in water-acetonitrile solutions. *Chem. Commun.* **2013**, *49*, 7767–7769.
- (27) Appel, A. M.; Pool, D. H.; O'Hagan, M.; Shaw, W. J.; Yang, J. Y.; Rakowski DuBois, M.; DuBois, D. L.; Bullock, R. M. $[Ni(P^{Ph}_2N^{Bn}_2)(CH_3CN)]^{2+}$ as an Electrocatalyst for H_2 Production: Dependence on Acid Strength and Isomer Distribution. *ACS Catal.* **2011**, *1*, 777–785.
- (28) Yang, J. Y.; Smith, S. E.; Liu, T.; Dougherty, W. G.; Hoffert, W. A.; Kassel, W. S.; DuBois, M. R.; DuBois, D. L.; Bullock, R. M. Two pathways for electrocatalytic oxidation of hydrogen by a nickel bis(diphosphine) complex with pendant amines in the second coordination sphere. *J. Am. Chem. Soc.* **2013**, *135*, 9700–9712.
- (29) Lense, S.; Dutta, A.; Roberts, J. A. S.; Shaw, W. J. A proton channel allows a hydrogen oxidation catalyst to operate at a moderate overpotential with water acting as a base. *Chem. Commun.* **2014**, *50*, 792–795.
- (30) Wilson, A. D.; Newell, R. H.; McNevin, M. J.; Muckerman, J. T.; DuBois, M. R.; DuBois, D. L. Hydrogen oxidation and production using nickel-based molecular catalysts with positioned proton relays. *J. Am. Chem. Soc.* **2006**, *128*, 358–366.
- (31) Das, P.; Ho, M.-H.; O'Hagan, M.; Shaw, W. J.; Bullock, R. M.; Raugei, S.; Helm, M. L. Controlling proton movement: electrocatalytic oxidation of hydrogen by a nickel(II) complex containing proton relays in the second and outer coordination spheres. *Dalton Trans.* **2014**, *43*, 2744–2754.
- (32) Lense, S.; Ho, M. H.; Chen, S. T.; Jain, A.; Raugei, S.; Linehan, J. C.; Roberts, J. A. S.; Appel, A. M.; Shaw, W. Incorporating amino acid esters into catalysts for hydrogen oxidation: steric and electronic effects and the role of water as a base. *Organometallics* **2012**, *31*, 6719–6731.
- (33) Dutta, A.; Lense, S.; Hou, J.; Engelhard, M.; Roberts, J. A. S.; Shaw, W. J. Minimal proton channel enables H_2 oxidation and production with a water soluble nickel-based catalyst. *J. Am. Chem. Soc.* **2013**, *135*, 18490–18496.
- (34) Dutta, A.; Roberts, J. A. S.; Shaw, W. J. Arg-Arg Pairing Enhances H_2 Oxidation Catalyst Performance. *Angew. Chem.* **2014**, *53*, 6487–6491.
- (35) Zhang, Z. Y.; Xu, Z. J.; Yang, Z.; Liu, Y. T.; Wang, J. A.; Shao, Q.; Li, S. J.; Lu, Y. X.; Zhu, W. L. The stabilization effect of dielectric constant and acidic amino acids on arginine-arginine (Arg-Arg) pairings: Database survey and computational studies. *J. Phys. Chem. B* **2013**, *117*, 4827–4835.
- (36) Kilgore, U. J.; Roberts, J. A. S.; Pool, D. H.; Appel, A. M.; Stewart, M. P.; Rakowski DuBois, M.; Dougherty, W. G.; Kassel, W. S.; Bullock, R. M.; DuBois, D. L. Studies of a series of $Ni(P^{Ph}_2N^{R_2})_2(BF_4)_2$ complexes as electrocatalysts for H_2 production: effect of substituents, acids, and water on catalytic rates. *J. Am. Chem. Soc.* **2011**, *133*, 5861–5872.
- (37) Pool, D. H.; Stewart, M. P.; O'Hagan, M.; Shaw, W. J.; Roberts, J. A. S.; Bullock, R. M.; DuBois, D. L. Acidic ionic liquid/water solution as both medium and proton source for electrocatalytic H_2 evolution by $[Ni(P_2N_2)_2]^{2+}$ complexes. *Proc. Natl. Acad. Sci. U.S.A.* **2012**, *109*, 15634–15639.
- (38) Jain, A.; Lense, S.; Linehan, J. C.; Raugei, S.; Cho, H.; DuBois, D. L.; Shaw, W. J. Incorporating peptides in the outer-coordination sphere of bioinspired electrocatalysts for hydrogen production. *Inorg. Chem.* **2011**, *50*, 4073–4085.
- (39) Jain, A.; Reback, M. L.; Lindstrom, M. L.; Thogerson, C. E.; Helm, M. L.; Appel, A. M.; Shaw, W. J. Investigating the role of the outer-coordination sphere in $[Ni(P^{Ph}_2N^{Ph-R_2})_2]^{2+}$ hydrogenase mimics. *Inorg. Chem.* **2012**, *51*, 6592–6602.
- (40) Reback, M. L.; Ginovska-Pangovska, B.; Ho, M.-H.; Jain, A.; Squier, T. C.; Raugei, S.; Roberts, J. A. S.; Shaw, W. J. The role of a dipeptide outer-coordination sphere on H_2 -production catalysts: influence on catalytic rates and electron transfer. *Chem.—Eur. J.* **2013**, *19*, 1928–1941.
- (41) Reback, M. L.; Buchko, G. W.; Kier, B. L.; Ginovska-Pangovska, B.; Xiong, Y.; Lense, S.; Hou, J.; Roberts, J. A. S.; Sorensen, C. M.; Raugei, S.; Squier, T. C.; Shaw, W. J. Enzyme design from the bottom up: an active nickel electrocatalyst with a peptide outer coordination sphere. *Chem.—Eur. J.* **2014**, *20*, 1510–1514.
- (42) Kier, B. L.; Shu, I.; Eidschink, L. A.; Andersen, N. H. Stabilizing capping motif for beta-hairpins and sheets. *Proc. Natl. Acad. Sci. U.S.A.* **2010**, *107*, 10466–10471.
- (43) Jain, A.; Buchko, G. W.; Reback, M. L.; O'Hagan, M.; Ginovska-Pangovska, B.; Linehan, J. C.; Shaw, W. J. Active hydrogenation catalyst with a structured, peptide-based outer coordination sphere. *ACS Catal.* **2012**, *2*, 2114–2118.
- (44) Shaw, W. J. The outer-coordination sphere: Incorporating amino acids and peptides as ligands for homogeneous catalysts to mimic enzyme function. *Catal. Rev.: Sci. Eng.* **2012**, *54*, 489–550.

(45) Silver, S. C.; Niklas, J.; Du, P.; Poluektov, O. G.; Tiede, D. M.; Utschig, L. M. Protein delivery of a Ni catalyst to photosystem I for light-driven hydrogen production. *J. Am. Chem. Soc.* **2013**, *135*, 13246–13249.